

Optical wavefront sensor based on sub-wavelength metallic structures

Riad Haïdar^a, Bruno Toulon^a, Grégory Vincent^{a,b}, Stéphane Collin^b, Sabrina Velghe^c, Jérôme Primot^a and Jean-Luc Pelouard^b

^a ONERA/DOTA, Chemin de la Hunière, F-91761 Palaiseau Cedex, France;

^b LPN/CNRS, route de Nozay, F-91460 Marcoussis, France;

^c Phasics, Campus Polytechnique, F-91128 Palaiseau, France.

ABSTRACT

Lateral shearing interferometers (LSIs) are efficient tools for optical analysis. They allow classical optical wavefront aberrations measurements as well as the precise evaluation of abrupt steps. The basic element of an LSI is the transmittance grating, which diffracts a number of orders (two in the case of a mono-dimensional LSI, ideally three or four non coplanar orders in the case of bi-dimensional LSI). This brings the need for specifically designed transmittance gratings. For instance, a mono-dimensional LSI needs a sinusoidal-shaped transmittance, since its Fourier transform carries exactly 2 orders. Such transmittances are however either impossible or at least extremely costly to design using classical *macroscopic* techniques, mainly because the usual thin film deposition techniques require several technological steps, in order to get the desired light filtering effect.

Given these constraints, we made use of sub-wavelength structures in order to build a new class of LSI. They are made of sub-wavelength lamellar metallic gratings specifically designed for the mid-infrared, and allow the precise coding of the desired transmission shape all over the LSI grating.

Keywords: Interferometry, sub-wavelength structures, optical analysis, infrared

1. INTRODUCTION

Optical metrology is a steady need in many fields of optical industry: imaging, laser, astronomy, ophthalmology... For years, many techniques have been proposed. Among them lateral shearing interferometers (LSIs) have proved powerful for laser beam evaluation and postprocessing, adaptive optics loops or classical optical testing. The principle of these interferometers is to superpose laterally shifted replicas of the wavefront under study; there is then no need of a reference surface, which is a great advantage in terms of compactness and setup simplicity.

An evolution of the classical LSI appeared in the laboratory of ONERA. It consists in the interference of more than two replicas of the impinging wave front; such interferometer is called multiple-wave LSI subsequently.^{1,2} The replicas are laterally shifted in different directions and interfere, which allows a wave front analysis for each direction. Originally, the concept was developed to measure the atmospheric turbulence-induced aberrations and improve the images of large telescopes by deconvolving them. However this kind of interferometer can be fruitfully used in many other fields: for example, they are, for long, successfully used for intense laser beam analysis and shaping;^{3,4} moreover four-wave LSI has recently been demonstrated to analyze discontinuous surfaces.⁵⁻⁷

In the following, we will first dwell on general considerations on multi-wave LSI and nano-structured gratings. As an example, we will then present the realization of metallic sub-wavelength structures designed to code various transmittance levels. Such structures can be used to make an improved quadri-wave LSI grating, and are shown to increase, in a non-negligible way, the optical performances of the gratings.

Contacts:

Riad Haïdar: haidar@onera.fr

2. MULTIPLE-WAVE LATERAL SHEARING INTERFEROMETRY

2.1 Concept

As suggested above, the first step to multiple-wave LSI is to make use of at least three replicas; these replicas can be generated by an optical system¹ or by Fourier filtering, of which the major drawback is the size. It appears that the use of one supplementary replica (leading to quadri-wave LSI, or QWLSI) allows to considerably simplify and reduce in size the replication device, at least in the concept: indeed, a simple grating⁸ can be used, which moreover ensures that the interferogram is achromatic.

A set of noticeable properties makes the multiple wave-LSI a powerful metrological tool. First of all, the redundancy of information enables a robust wavefront evaluation;⁹ indeed each couple of replicas leads to a derivative. Moreover, the error made in the phase derivative evaluation can be estimated, thanks to a closure relation in the gradients.¹ Moreover the use of a grating as replication device allows to design compact interferometers. Finally the sensitivity is adjustable by moving the grating from the observation plan: the deformations of the interferogram depend on the propagation distance, *ie* on the distance between the grating and the observation plane.

2.2 Classical design of the QWLSI grating

The ideal QWLSI grating would diffract exactly four orders, *ie* it is a bi-dimensional sinusoidal transmittance. However so far, such a transmittance is difficult to realize, using classical deposition techniques. An approximation was thus proposed: instead of coding a perfectly sinusoidal transmittance, a three-level (+1, 0 and -1) approximation was made. A period of the transmittance is illustrated on Fig. 1. It can be seen as the well-known Hartmann mask completed by a phase chessboard; that is why it is called Modified Hartmann Mask, or MHM.⁸

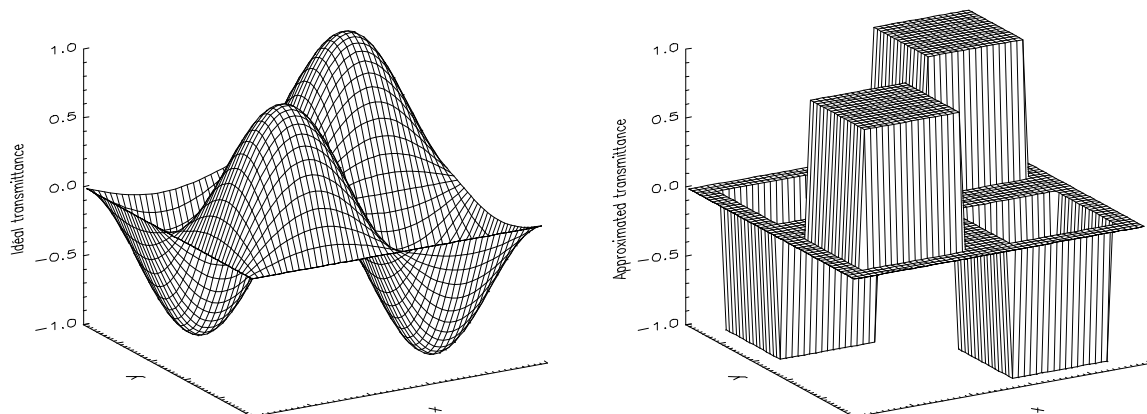


Figure 1. Approximation of the perfect, ideal sinusoidal transmittance by a three-level transmittance (MHM).

The approximation MHM is easily made using classical techniques: the +1-level corresponds to the bare substrate, the 0-level is obtained by an opaque metal deposit, and the -1-level corresponds to a phase of π over the bare substrate. The later can be coded by etching a thickness $e = \frac{\lambda}{2(n-1)}$ of the substrate so as to produce the right phase step. This results in a grating diffracting four preponderant orders but also parasitic orders, which can be reduced by advantageously choosing the area of each domain.⁸

However these parasitic orders, even reduced, still pollute the diffraction pattern and thus the measurement. It seems then necessary to get a better approximation of the desired transmittance.

2.3 Nano-structured grating

We propose the use of hybrid dielectric/metallic sub-wavelength structures to design a diffractive device for LSI in the mid-infrared wavelength range. A key element is the ability to code any transmission intensity. Such a grey-scale transmission coding can be obtained with metallic gratings structured at the sub-wavelength scale. In the following section, we show how metallic nanostructures allow to design a discrete-levels transmittance pattern. Each level (or *domain*) of the transmittance is obtained with a sub-wavelength grating with a dedicated geometry. Then we analyze the influence of the additional phase induced by metallic nanostructures, and we propose to compensate this phase shift with a complementary stepped phase grating. We show that these techniques result in the quasi-total suppression of parasitic diffracted waves.

As an illustrative realization, we focus on the particular case of a QWLSI grating, which ideally consists in a bi-dimensional sinusoidal transmittance. Then, a comparison with an existing system (the classical MHM described above) will provide useful information on the pertinence of the nano-structuration approach, which may in turn be implemented for the realization of more complex transmittances.

3. NANO-STRUCTURE BASED GRATING

3.1 Coding optical transmittance with sub-wavelength gratings

We aim to design a transmittance $\tau(x) = t(x) \exp(i\psi(x))$ pattern coded both in module t and in phase ψ . For a good approximation of the desired shape, the function $t(x)$ is divided into a number of domains of uniform transmission level t_n . Each transmission value t_n is coded with a sub-wavelength metallic grating having a specific geometry and the phase ψ_n is coded using a dielectric grating. The gratings are then put side-by-side to reconstruct the desired pattern. As an example, Fig. 2 illustrates the case of the modulus value t of a sinusoidal pattern coded on five levels.

Each transmission level t_n is obtained with a lamellar sub-wavelength metallic grating. The thickness of the metallic layer is kept constant all through the device, and each level t_n is obtained by adjusting the grating period and/or the slits width.

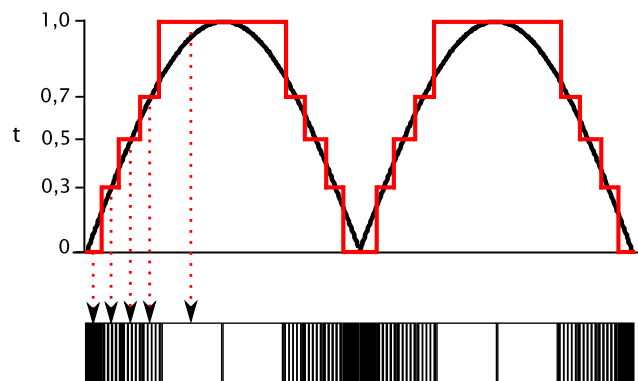


Figure 2. Example of a sinusoidal transmittance, approximated by a few sub-wavelength gratings per period. Each grating n codes a transmittance level t_n .

Optical transmittances through metallic gratings are calculated using a quasi-analytical one-mode model widely studied in the literature.^{10,11} It allows a fast study of metallic gratings with a wide range of geometrical parameters (h , w and d , Fig. 3), and provides a simple understanding of physical mechanisms involved in the transmission process. This model is valid as far as the metal thickness h and the slits width w fulfil the following conditions (i) each slit behaves as a one-mode metallic planar waveguide, *ie* the only guided mode is the TM_0 mode ($w < \lambda/2$),¹² (ii) other (evanescent) modes in the slits are sufficiently attenuated and can be neglected ($h > w/\pi$).¹⁰ As a consequence, the whole structure transmits only TM (transverse magnetic, *ie* magnetic field parallel to the grating slits) polarized waves, whereas TE (transverse electric) waves are totally back-reflected.

As shown on Fig. 4, it is possible to code any value of transmission t between 0 and $\simeq 1$ by adjusting the value of the slit width w . However, as pointed out in Ref. 13, 14, and shown on Fig. 4, the use of metallic

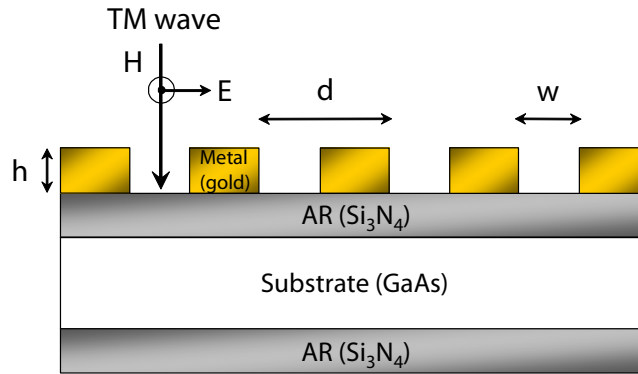


Figure 3. Definition of the geometrical parameters of the gratings (d , h and w). The substrate is double-side anti-reflection (AR) coated.

gratings induces an additional phase $d\psi$ in each domain, which can be compensated by using complementary dielectric gratings, as will be shown further.

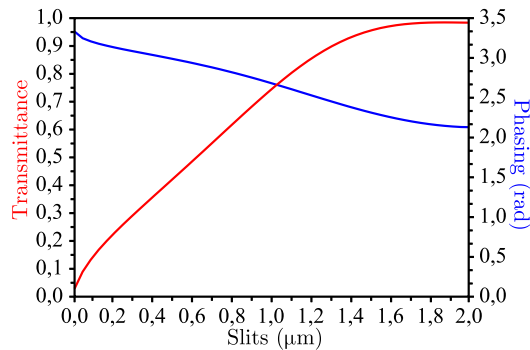


Figure 4. Module t (red) and phase $d\psi$ (blue) of the transmittance τ as a function of the grating slit w . The period is $d = 2 \mu\text{m}$ and the height is $h = 500 \text{ nm}$.

The following section describes a typical technological process for the realization of a sub-wavelength structured grating for the infrared.

3.2 Fabrication process

The basic structure is made of a gold grating deposited on a gallium arsenide (GaAs) substrate, which is first double-side anti-reflection (AR) coated (Fig. 3). The whole structure is designed for the mid-infrared. As a consequence, the AR-layers and the gratings have been optimized for a wavelength of $\lambda = 7 \mu\text{m}$. The period d and the gold thickness h are chosen in order to avoid the apparition of diffracted waves in the air and in the substrate and to fulfil the above conditions (i) and (ii): $d = 2 \mu\text{m}$ and $h = 0.5 \mu\text{m}$. The transmission intensity is then simply a function of the slit width w . The result of the five-level transmission optimization is shown in Table 1. For each grating width, the calculated transmittance and phase are provided. The zero and maximum transmission levels are obtained with an opaque metal film and without metallic structures, respectively.

The metallic gratings are defined by electron-beam lithography in a $1 \mu\text{m}$ -thick PMMA (poly(methyl metacrylate)) layer. After resist development, titanium/gold (3nm/500nm) layers are deposited by electron-beam assisted evaporation and lifted off in acetone. The thin titanium layer is used to improve the gold adhesion. This layer is expected not to affect the transmission properties of the structure, since no strong field enhancement occurs close to this metal-dielectric interface.

It was recently shown¹³ that it is possible to code various transmittance levels (between 13% and 93% in intensity) with a good accuracy. Moreover, the test component of Ref. 13,15 was shown to provide a wide spectral tolerance (typically, over the $5 - 8 \mu\text{m}$ spectral region), which may be of some use for imagery applications.

| Grating | 1 | 2 | 3 | 4 | 5 |
|--------------------------------------------|----------|---------------------------------|-------------------------------|---------------------------------|-------|
| Slits width w_n (nm) | 0 | 310 | 620 | 930 | 2000 |
| Period d (μm) | 2 | 2 | 2 | 2 | 2 |
| Thickness h (nm) | 500 | 500 | 500 | 500 | 500 |
| Calculated transmission t_n (%) | 0 | 30 % | 50 % | 70 % | 100 % |
| Calculated parasitic phase $d\psi_n$ (rad) | \times | $0.950 \approx \frac{\pi}{3.3}$ | $0.796 \approx \frac{\pi}{4}$ | $0.600 \approx \frac{\pi}{5.2}$ | 0 |

Table 1. This table summarizes the geometry of the gratings for each transmittance level. Gratings are deposited on a GaAs substrate with silicon nitride (Si_3N_4) anti-reflection layers. Thicknesses are: 850nm/300 μm /850nm for $\text{Si}_3\text{N}_4/\text{GaAs}/\text{Si}_3\text{N}_4$ (optical indexes at 7 μm : 2.05/3.28/2.05).

3.3 A sinusoidal transmittance pattern

The previous five levels of transmission t_n (Table 1) can be used to build a 9-level approximation of a sinusoidal transmittance pattern – four levels for the positive arch of the transmittance τ , another four for the negative arch and one level for the zero transmittance. Let's point out that for the negative arch, the sign is coded by superposing a phase pattern, which periodically adds a $\Psi = \pi$ phase shift (Fig. 5), thus periodically reversing the sign of the transmittance. This phase pattern can be simply achieved by etching the substrate on a depth of $\frac{\lambda}{2(n-1)}$. But, as already pointed out in Table 1 and illustrated on Fig. 6, metallic gratings induce an additional parasitic phase shift $d\psi$, which can have dramatic consequences on the diffraction pattern of the LSI grating. This parasitic phase was measured thanks to QWLSI¹⁴ and was found to be in good agreement with calculations. Typically, phase variations between 0 and $\pi/2$ radians are observed, depending on the slit width w , which may distort the transmittance pattern.

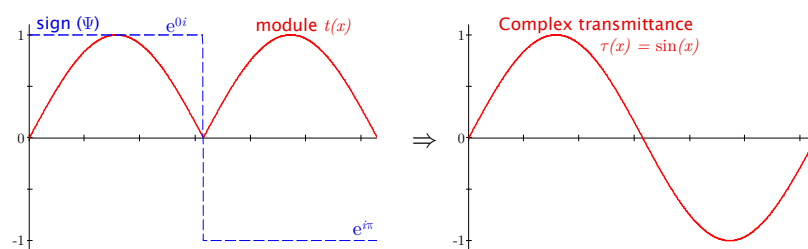


Figure 5. The transmittance $\tau = \sin(x)$ can be coded by the multiplication of $|\sin(x)|$ in transmission and a sign function ($\exp(\pi i)$ or $\exp(0i)$) coded in phase.

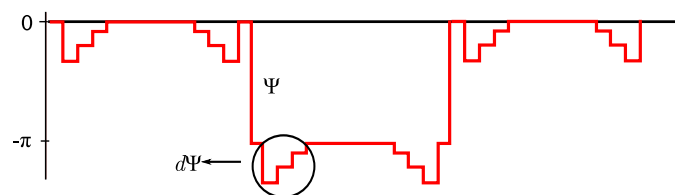


Figure 6. Illustration of the parasitic phase $d\psi$ introduced by each sub-wavelength grating.

More precisely, simulations undoubtedly show that the influence of the parasitic phase is the primary quality criterion of the LSI grating, much more than the choice (number and amplitude) of the transmission levels t_n . As proposed in Ref. 13, one may compensate for this additional phase $d\psi$ by the use of an additional etching of the substrate. Indeed, the influence of the parasitic phase shift of the approximated transmittance pattern is estimated with a propagation-pattern analysis of the complex transmitted amplitude, as illustrated on Fig. 7. A perfect sinusoidal transmittance (Fig. 7a) diffracts exactly two orders: as a consequence, the diffracted wave propagates along perfect light-pipes. Fig. 7b and 7c show the results obtained with a 9-level approximation

of the sinusoidal transmittance, respectively without and with a compensation of the parasitic phase due to the metallic gratings. This phase compensation consists in a simple etching of the substrate, so that only one parasitic phase level is totally corrected. This solution is a good compromise between technological complexity and the technical performance required. Indeed, propagation pattern demonstrates that this phase compensation is sufficient to efficiently extinct the main parasitic orders: the light-pipes are nearly perfectly recovered.

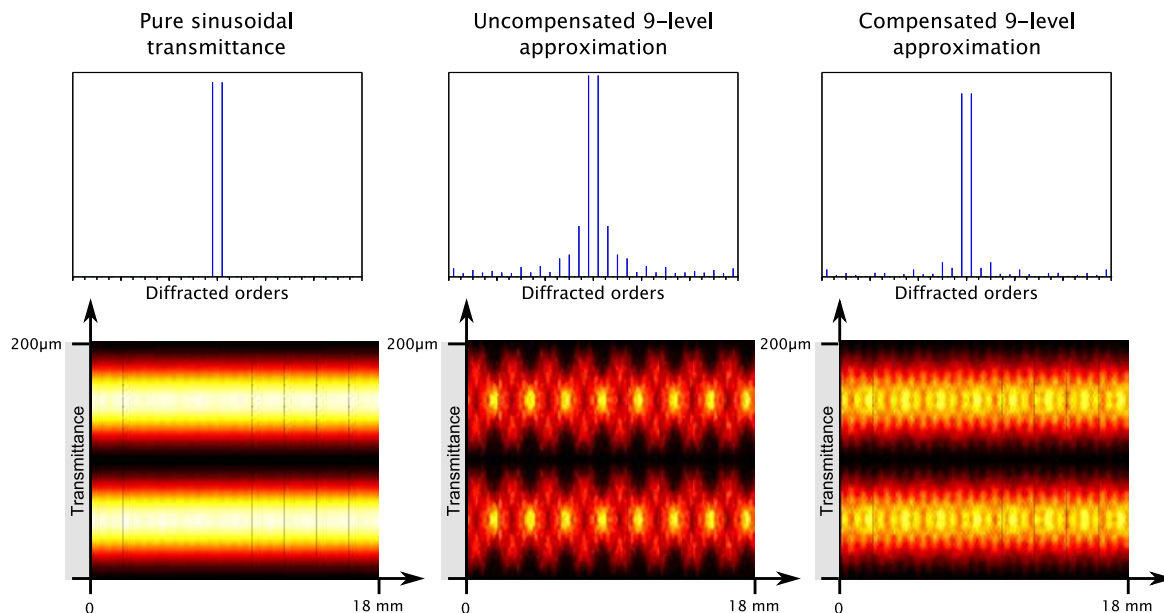


Figure 7. Comparison between the perfect sinusoidal transmittance (a) and the 9-level approximation. In case (b) the parasitic phase $d\psi$ are uncompensated whereas in case (c), only the greatest parasitic phase is.

4. QWLSI NANOSTRUCTURED GRATING

We make use of the previously demonstrated structure to design a 2D mask approximating a 2D sinusoidal transmittance pattern. The various domains are put side-by-side in order to reconstruct a discrete, 9-transmission-level approximation, with one level of phase compensation, that we call enhanced-MHM (eMHM).

For a comparison purpose, a schematic diagram of the eMHM is given on Fig. 8, which also shows the diffraction spectra of both MHM and eMHM. As can be seen, the spectrum of the eMHM contains much less parasitic orders, which proves that the eMHM provides a better approximation of the desired sinusoidal pattern.

In order to quantitatively evaluate the quality of the diffracted pattern, one may introduce a criterion¹³ defined as the ratio f between the amplitude of the strongest parasitic order C_{max} and the amplitude of the first order C_1 : $f = C_{max}/C_1$. The strength of the parasitic modulations of the light pipes is directly linked to this quality criterion. The criterion is null for the ideal sinusoidal pattern. One can calculate that $f = 0.202$ for the MHM, and decreases to $f = 0.079$ for the eMHM.

5. CONCLUSION

It was shown that sub-wavelength metallic structures can answer growing needs in the field of diffracting masks for optical analysis systems. They allow to modulate the transmittance pattern on a tiny scale, and thus to realize qualitative approximations of any transmissive mask.

As discussed and shown in the paper, sub-wavelength structures can code both the module and the phase of the transmittance pattern. So far, the phase coding appears as a parasitic phenomenon, which can be compensated for by the use of an additional phase grating (obtained e.g. by a simple etching of the substrate). However,

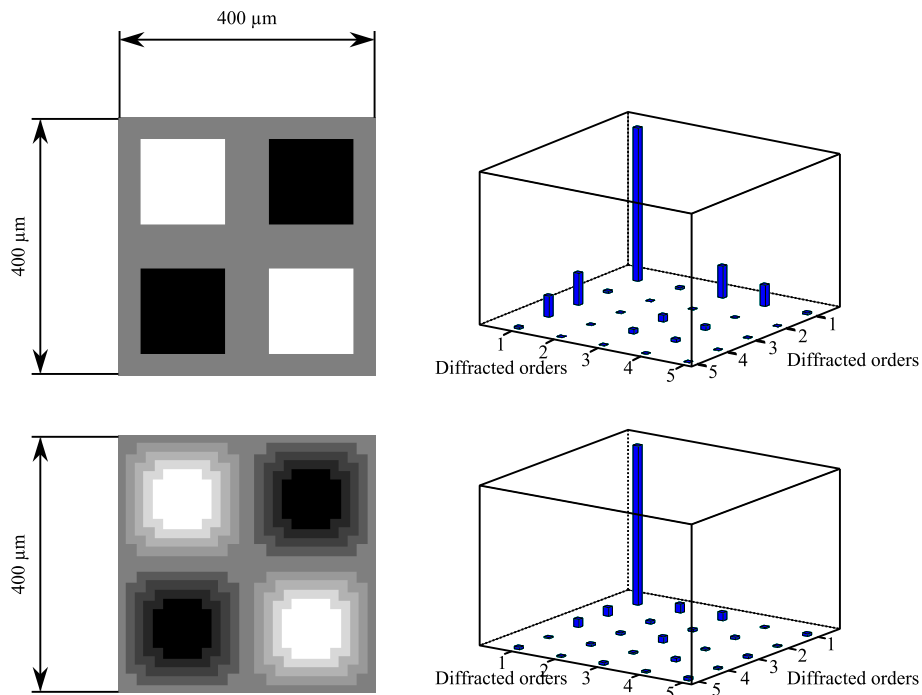


Figure 8. Comparison between a MHM and a eMHM. The transmittances (left) are schematized with their related spectra (right; notice that only a quarter of the Fourier space is represented).

the deterministic and simultaneous coding of both module and phase using sub-wavelength structures is under investigation.

In conclusion, a first prototype of the eMHM is currently in process, and first experimental tests and results will be published soon.

REFERENCES

- [1] Primot, J., “Three-wave lateral shearing interferometer,” *Appl. Opt.* **32**, 6242–6249 (1993).
- [2] Primot, J. and Sogno, L., “Achromatic three-wave (or more) lateral shearing interferometer,” *J. Opt. Soc. Am. A* **12**, 2679–6285 (1995).
- [3] Chanteloup, J. C., Druon, F., Nantel, M., Maksimchuk, A., and Mourou, G., “Single-shot wave-front measurements of high intensity ultrashort laser pulses with a three-wave interferometer,” *Opt. Lett.* **23**, 621–623 (1998).
- [4] Druon, F., Cheriaux, G., Faure, J., Nees, J., Nantel, M., Maksimchuk, A., Mourou, G., Chanteloup, J., and Vdovin, G., “Wave-front correction of femtosecond terawatt lasers by deformable mirrors,” *Opt. Lett.* **23**, 1043–1045 (1998).
- [5] Chanteloup, J.-C., “Multiple-wave lateral shearing interferometry for wave-front sensing,” *Appl. Opt.* **44**, 1559–1571 (2005).
- [6] Toulon, B., Primot, J., Guérineau, N., Haïdar, R., and Velghe, S., “Segmented wave-front measurements by lateral shearing interferometry,” in [*Optics and Photonics*], *Proc. SPIE* **6671** (2007).
- [7] Toulon, B., Primot, J., Guérineau, N., Haïdar, R., Velghe, S., and Mercier, R., “Step-selective measurement by grating-based lateral shearing interferometry for segmented telescopes,” *Opt. Commun.* **279**, 240–243 (2007).
- [8] Primot, J. and Guérineau, N., “Extended hartmann test based on the pseudoguiding property of a hartmann mask completed by a phase chessboard,” *Appl. Opt.* **39**, 5715–5720 (2000).
- [9] Velghe, S., Primot, J., Guérineau, N., Cohen, M., and Wattellier, B., “Wave-front reconstruction from multidirectional phase derivatives generated by multilateral shearing interferometers,” *Opt. Lett.* **30**, 245–247 (2005).
- [10] Lalanne, P., Hugonin, J., Astilean, S., Palamaru, M., and Möller, K., “One-mode model and airy-like formulae for one-dimensional metallic gratings,” *J. Opt. A: Pure Appl. Opt.* **2**, 48–51 (2000).
- [11] Barbara, A., Quémerais, P., Bustarret, E., and Lopez-Rios, T., “Optical transmission through subwavelength metallic gratings,” *Phys. Rev. B* **66**(16), 161403 (2002).
- [12] García-Vidal, F. J. and Martín-Moreno, L., “Transmission and focusing of light in one-dimensional periodically nanostructured metals,” *Phys. Rev. B* **66**(15), 155412 (2002).
- [13] Vincent, G., Haidar, R., Collin, S., Guérineau, N., Primot, J., Cambril, E., and Pelouard, J.-L., “Realization of sinusoidal transmittance with subwavelength metallic structures,” *J. Opt. Soc. Am. B* **25**(5), 834–840 (2008).
- [14] Toulon, B., Vincent, G., Haidar, R., Guérineau, N., Collin, S., Pelouard, J.-L., and Primot, J., “Holistic characterization of complex transmittances generated by infrared sub-wavelength gratings,” *Opt. Express* **16**, 7060–7070 (2008).
- [15] Vincent, G., Haïdar, R., Collin, S., Cambril, E., Velghe, S., Primot, J., Pardo, F., and Pelouard, J.-L., “Complex transmittance gratings based on subwavelength metallic structures,” in [*Nanophotonics*], *Proc. SPIE* **6195** (2006).